

Contents list available at **IJND**  
**International Journal of Nano Dimension**

Journal homepage: [www.IJND.ir](http://www.IJND.ir)

---

## Incorporation of 12-Tungstophosphoric acid in Titania spheres and fabrication of core-shell Polyoxotungstate/Titania nanostructures

---

### ABSTRACT

**M. Seyedsadjadi<sup>1,\*</sup>**  
**S. Rashidzadeh<sup>1</sup>**  
**N. Farhadyar<sup>2</sup>**

<sup>1</sup>Department of chemistry,  
Science and Research Branch,  
Islamic Azad University, Tehran,  
Iran.

<sup>2</sup>Department of Chemistry,  
Varamin -Pishva Branch,  
Islamic Azad University,  
Varamin, Iran.

Received: 18 June 2012

Accepted: 28 September 2012

Core-shell 12-tungstophosphoric acid/TiO<sub>2</sub> (HPW/TiO<sub>2</sub>) nanoparticles at 10 and 20% of HPW have been synthesized by simple in-situ sol- gel method. Characterization of the samples was carried out by X-ray diffraction (XRD), Scanning electron microscopy (SEM), Fourier transform infrared (FTIR). The X-ray diffraction patterns of as prepared solid samples, indicated characteristic peaks of titania with additional peaks concerning to HPW in a very low intensities. This result in addition to the FTIR and SEM - EDX analysis data confirmed incorporation of HPW / TiO<sub>2</sub> nanostructure in spherical morphology with a particle size of around 25 nm.

**Keywords:** *Polyoxometalates; Phosphotungstic acid; Keggin type structure; Inorganic-inorganic nanostructure; Titania phase.*

---

### INTRODUCTION

Polyoxometalates (POMs) are a large class of compounds that have been extensively used as acid and oxidation catalysts in many reactions, notably because their acid-base and redox properties that can be tuned by simple change in the polyanion chemical composition [1-4]. Among the numerous POMs, Keggin type POMs such as polyoxotungstates (PW) have been attractive because of their strong bronsted acid properties, exhibition of fast reversible multi electron redox behavior under mild conditions, tunable redox properties and also easy access [5]. Unfortunately, these compounds are highly soluble in various polar solvents which cause problems in separation from reaction media and render them less attractive for applications in heterogeneous catalysis. Among the different protocols proposed to solve problem, immobilization of polyoxometalates on porous oxide materials seems very cheap, attractive and practicable [6, 7].

---

\* Corresponding author:  
Prof.Mirabdollah Seyedsadjadi  
Department of chemistry, Science  
and Research Branch, Islamic  
Azad University, Tehran, Iran.  
Tel +96 479 01793866  
Fax +96 479 01793866  
Email [m.s.sadjad@gmail.com](mailto:m.s.sadjad@gmail.com)

To date, it has been shown that supporting POMs into the suitable inorganic solids such as carbon, silica, titania and etc [7-9] have good supporting properties which are effective method to overcome the mentioned problem [10-14]. In this work, successful preparation and characterization of polyoxotungstate nanostructure incorporated with TiO<sub>2</sub> (HPW/TiO<sub>2</sub>) have been reported.

## EXPERIMENTAL

### Material and characterization

All chemicals and solvents were purchased from Merck or Fluka and used as received without further purification. Samples were characterized with FTIR, UV-Vis, SEM and X-ray powder diffraction. The secondary electron micrographs of the samples were obtained to obtain the shape and diameter of particles by scanning electron microscopy (SEM), using Philips Model 505 equipment, at a working potential of 15 kV, and samples coated with gold. Crystalline phase characterization was carried out by the powder X-ray diffraction (XRD) patterns were collected on Rigaku Miniflex diffractometer using Cu K $\alpha$  radiation ( $\lambda = 0.1541$  nm,  $k=0.94$ ), nickel filter, in the high voltage source 40 kV, 30 mA, and scanning angle between  $2\theta = 10 - 90^\circ$  at a scanning rate of 18/min. Fourier transform infrared (FTIR) spectra were recorded on a Thermo Nicolet spectrometer using KBr disc method in the 400–4000 cm<sup>-1</sup> wavenumber range. The UV-vis spectra were recorded in the 400–4000 nm range on a Perkin-Elmer Lambda 35 apparatus.

### Nanomaterials synthesis

- *Synthesis of nTiO<sub>2</sub>*

Titanium tetraisopropoxide (TTIP) (0.0125 mol) was added dropwise to a molar mixture of EtOH/H<sub>2</sub>O and stirred vigorously at room temperature. The sol sample obtained by the hydrolysis process was then irradiated with ultrasonic equipment in an ultrasonic cleaning bath for 1 h and aged in closed beaker at room temperature for 24 h in order to obtain further hydrolyze of TTIP and mono dispersed TiO<sub>2</sub> nanoparticles. The sample obtained was finally dried at 100 °C for about 8 h in air to vaporize

water and alcohol from the gel and grounded to the fine powder after calcination at 400 °C in air for 1h.

- *Synthesis of PW nanoparticles*

Sodium tungstate (0.305mol) and disodiumphosphate (0.09 mol) were dissolved in boiling water (150 ml) and stirred magnetically. A concentrated hydrochloric acid (80 ml) was then added drop wise to the solution obtained and cooled. To separate impurity from the solution, some amount of ether was added and the lower part of solution was separated and evaporated to dryness mildly heating under air current.

- *Synthesis of PW / TiO<sub>2</sub> nanocomposite (First attempt (FA))*

The core shell PW-TiO<sub>2</sub> nanopowders was synthesized on the basis of sol-gel method reported in literature for preparation of some titania supported PW nanoparticles [15]. A solution of tetrabutyl orthotitanate in n-BuOH (25 mL) was prepared and stirred at 80 °C. The mixture was then slowly cooled to room temperature and adjusted to pH= 2 by using hydrochloric acid and was added a solution containing sodium tungstate (0.305 mole) and disodiumphosphate (0.09 mole). The mixture was then maintained under constant stirring rate for 3 h until occurrence of gelling process. The gel obtained was filtered and dried in air at 100 °C for 24 h and finally calcined in vacuum at 350 °C for 4 h to fasten the titania network and washed with hot water (80 °C) three times.

- *Synthesis of HPW/TiO<sub>2</sub> nanocomposite (Direct synthesis method)*

- *Synthesis of HPW/TiO<sub>2</sub> nanocomposite (Second Attempt (SA))*

Suitable amount of Sodium tungstate dihydrate and disodium hydrogen phosphate dodecahydrate were added to 75 ml of DI water and the mixture was stirred at 80 °C for 1 h. Then appropriate amount of nano TiO<sub>2</sub> (nTiO<sub>2</sub>) (in 10 and 20 wt % ) were added to solution. After then the mixture was stirred at 80 °C for 9 h and 82 ml of HCl solution was added drop wisely and mixed for 3 h at 80 °C. The precipitate was separated from mixture after 3 h at room temperature and then poured into petri dish and placed in convection oven overnight at 100 °C. afterward the powder

was ground to fine particles and dried at 130 °C for 6 h in oven.

#### - Synthesis of HPW/TiO<sub>2</sub> nanocomposite (Third attempt (TA))

Suitable amount of disodium hydrogenphosphate dodecahydrate and nano TiO<sub>2</sub> for 10 and 20 %wt were added to 75 ml of DI water and the mixture was stirred at 80 °C for 1 h. Then appropriate amount of sodium tungstate dihydrate for above weight percent were added to solution. After then the mixture was stirred at 80 °C for 9 h and 82 ml of HCl solution was added drop wisely and mixed for 3 h at 80 °C. The precipitate was separated from mixture after 3 h at room temperature and then poured into petri dish and placed in convection oven overnight at 100 °C. afterward the powder was ground to fine particles and dried at 130 °C for 6 h in oven.

## RESULTS AND DISCUSSION

### SEM micrographs and Dispersive X-RAY analysis (EDAX)

Figure 1a shows SEM micrograph of well spherically distributed TiO<sub>2</sub> nanoparticles prepared by the second method in this work. Particle size estimated through this image was lower than 50 nm. Figure 1b represents SEM images of TiO<sub>2</sub> nanoparticles loaded with 20 w% of PW nanoparticles. Interesting point taken from these images was the particle size diminution in incorporated nanostructures by increasing PW amounts and remaining spherical morphology in both the cases. The X-ray dispersive analysis (EDX) of the samples prepared in the second method shown in Table 1, confirms appropriate percentage values of P and W incorporated in TiO<sub>2</sub> nanostructures.

**Table 1.** EDX ZAF quantification (standardless) elements of nanocomposites prepared in second synthesis method

Sample	%P	%W	%O	%Ti	%Au
10%wt.-nHPW/n-TiO <sub>2</sub>	0.86	6.31	41.5	40.39	10.94
20%wt.-nHPW/n-TiO <sub>2</sub>	1.29	8.46	36.31	40.0	14.31

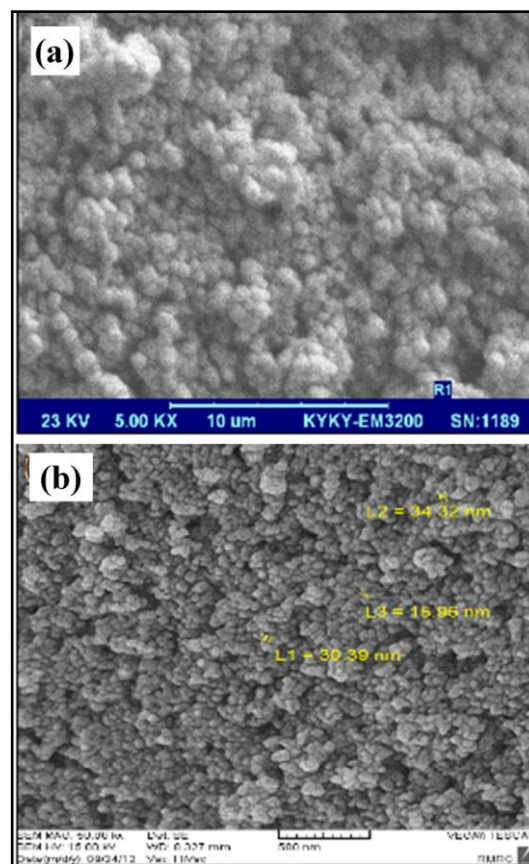


**Fig. 1.** a) TiO<sub>2</sub> nanoparticles; b) TiO<sub>2</sub> nanoparticles loaded by 20 % wt. of PW in second method (SA)

### X-ray diffraction

Figure 2 displays XRD diffraction pattern of TiO<sub>2</sub> nanoparticles synthesized in this work. It consists of a mixture of anatase and rutile phases. The peaks appeared at  $2\theta = 25, 38.0, 48.0$  and  $54.3^\circ$  elucidate the diffractions of the (101), (004), (200) corresponding to the anatase TiO<sub>2</sub> phase (JCPDS no. 21-1272). The other additional peaks observed with a low intensities at (110) and (200) reflections, can be indexed to hexagonal lattice crystallinities of TiO<sub>2</sub> rutile phase (JCPDS no 77-0441) [16]. The average crystalline size from the most intense anatase peak was estimated to be 50 nm using Scherrer's formula:

$$D = 0.9\lambda / \beta \cos\theta$$

Where ' $\lambda$ ' is wave length of X-Ray (0.1541 nm), ' $\beta$ ' is FWHM (full width at half maximum), ' $\theta$ ' is diffraction angle and ' $D$ ' is particle diameter size.

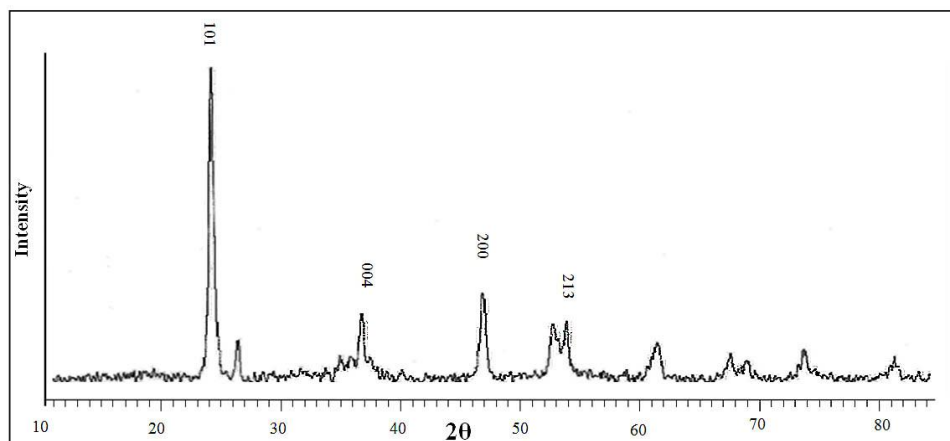


Fig. 2. XRD powder diffraction pattern of prepared nano  $\text{TiO}_2$

Figure 3 Shows XRD powder diffraction pattern obtained for synthesized HPW with the characteristic peaks of polyoxotungstate having Keggin structure [17]. The peaks appeared in this figure corresponded to the plane (101), (004), (200) and (213) are in conformity with the formation of crystalline Keggin structure in the synthesized samples (JCPDS file No. 50-0305). The average crystalline size calculated from Scherrer's formula using the most intense peak was estimated to be around 18 nm.

Figure 4<sub>(A,B,C)</sub> represent powder X-ray diffraction patterns of HPW,  $n\text{TiO}_2$  in comparison with HPW/ $\text{TiO}_2$  nanostructures incorporated with

10% wt. and 20 wt. % of HPW prepared in the first, second and third method. All X-ray diffraction patterns showed characteristic peaks of titania with additional peaks of HPW in a very low intensities showing formation of inorganic-inorganic composites or the presence of well dispersed of very small size of Keggin in or on the titania surface. The average particle size of as prepared nanocomposites prepared in the first, second and third method determined according to the Scherrer equation, are listed in Table 2. These data clearly indicated formation of core-shell nanostructured HPW/ $\text{TiO}_2$  in all the cases.

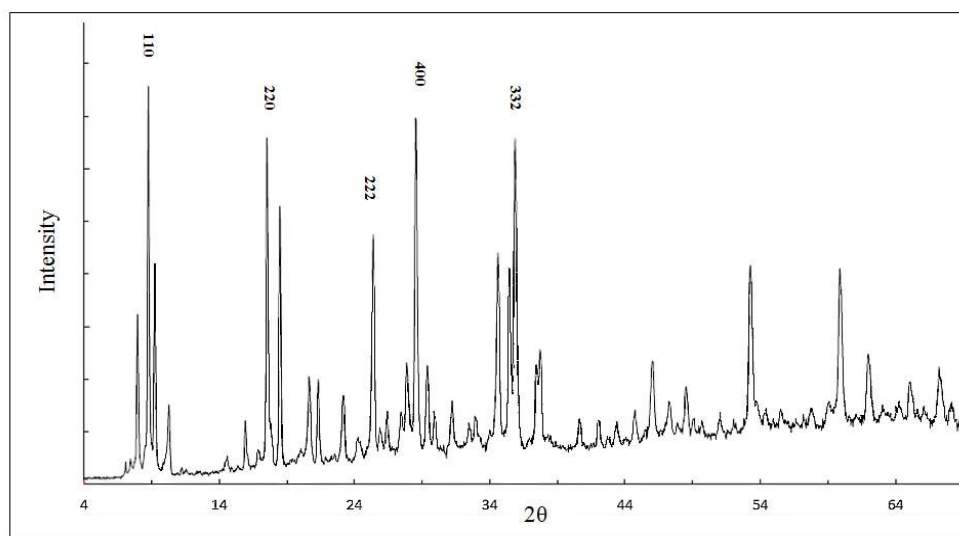
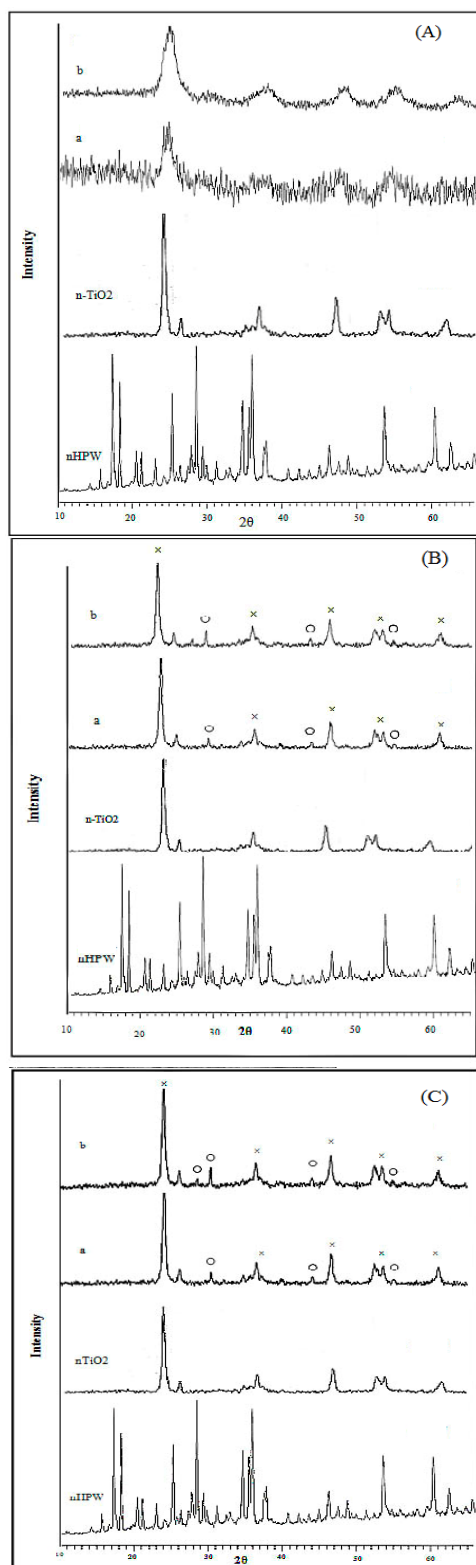


Fig. 3. XRD Pattern of nano HPW



**Fig. 4.** (A,B,C). XRD powder diffraction patterns of nTiO<sub>2</sub> incorporated with: a) 10% wt.nHPW; b) 20% wt. of nHPW prepared in first (A), second (B) and third method (C).

- i. Titania peaks are shown by ×
- ii. HPW peaks are shown by ○

**Table 2.** Crystalline size of synthesized nanocomposites

Sample	Crystallite Size(nm)
Nano TiO <sub>2</sub>	50
Nano HPW	18
10% wt.-nHPW/n-TiO <sub>2</sub> (a)	5.0
20% wt.-nHPW/n-TiO <sub>2</sub> (a)	10
10% wt.-nHPW/n-TiO <sub>2</sub> (b)	14
20% wt.-nHPW/n-TiO <sub>2</sub> (b)	15
10% wt.-nHPW/n-TiO <sub>2</sub> (c)	15
20% wt.-nHPW/n-TiO <sub>2</sub> (c)	16

### FTIR Spectra

Figures 5 (left, right) show FTIR spectra of nHPW/nTiO<sub>2</sub> samples prepared through the above mentioned methods with 10%wt. and 20 %wt. of HPW. In these Figures, infrared spectrum of the prepared HPW is included for comparative purposes. It has been widely reported that HPW with Keggin structures gives several strong typical IR bands assigned to HPW as follow: 1080 cm<sup>-1</sup> (stretching frequency of P–O in the central PO<sub>4</sub> tetrahedron), 987 cm<sup>-1</sup> (terminal bands for W O in the exterior WO<sub>6</sub> octahedron), 888 cm<sup>-1</sup> and 805 cm<sup>-1</sup> (bands for the W–O<sub>b</sub>–W and W–O<sub>c</sub>–W bridge and corner respectively) [18]. The FTIR results obtained for TiO<sub>2</sub> and TiO<sub>2</sub> supported nHPW samples with 10 and 20% wt HPW (Figures 5 L, R) showed typical bands for anatase phase at 700 cm<sup>-1</sup> which is in good accordance with reported data and the peaks appeared in the range from 1100 cm<sup>-1</sup> to 700 cm<sup>-1</sup> can be ascribed to the stretch vibrations of P–O, W- O, and W–O–W bonds of the Keggin units respectively, indicating that the primary Keggin structures of these polyoxotungstates remain intact. *Distinct shifting* characteristic peaks of HPW incorporated nanostructures different percent of nPW on TiO<sub>2</sub>, (10% wt. n-HPW/nTiO<sub>2</sub>) to a higher frequency (Figure 5), shows occurrence and formation of new chemical linkage between terminal W- O, and W–O–W bonds with loaded TiO<sub>2</sub> component. Interesting point is that, remaining of the peak corresponding to the stretching frequency of P–O in the central PO<sub>4</sub> tetrahedron and the peak at 987 cm<sup>-1</sup> (terminal

bands for WO in the exterior WO<sub>6</sub> octahedron) without any frequency shifting due to the linkage in TiO<sub>2</sub> supported HPW (Figure 5 right). This result in accordance with other published data can be due to the protection of WO<sub>6</sub> octahedron Keggin structure in TiO<sub>2</sub> supported HPW [19].

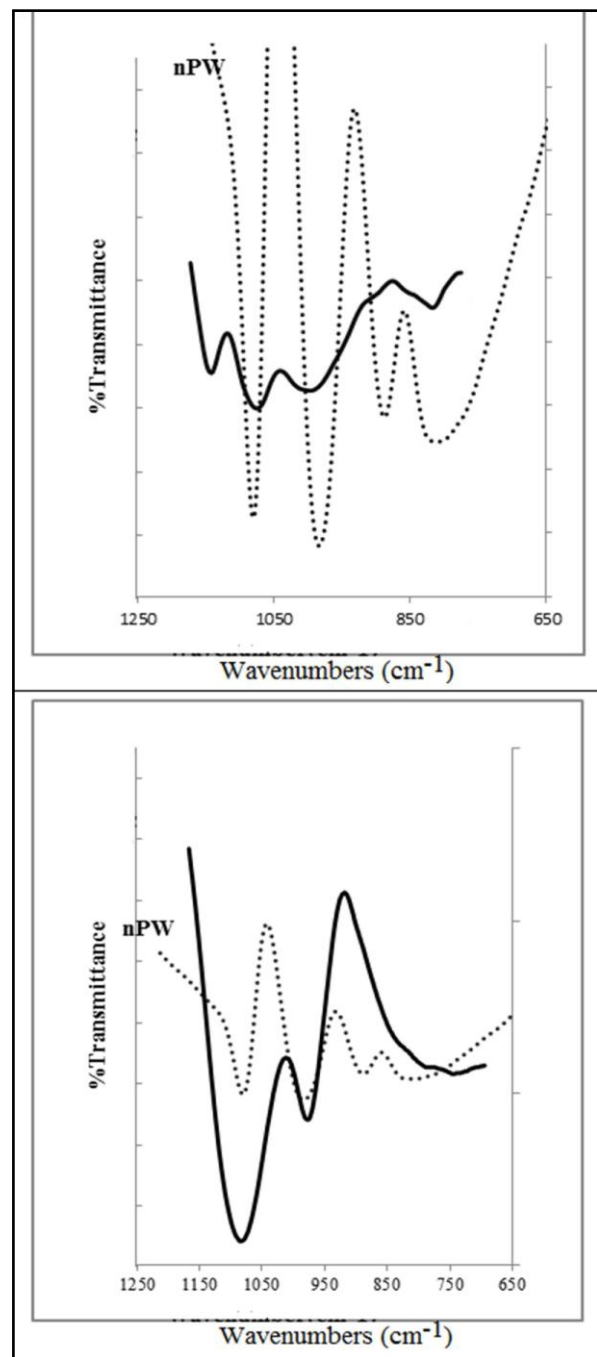


**Fig. 5.** FTIR Spectra of: Left) 10% nPW/TiO<sub>2</sub>; right) 20% nPW/TiO<sub>2</sub>. i. FTIR of PW showed as dashed line

## CONCLUSIONS

We successfully prepared core shell HPW/TiO<sub>2</sub> nanostructure with various content of HPW (10 and 20 wt. %), by in situ sol-gel method. The X-ray diffraction patterns showed characteristic peaks of titania with additional peaks of HPW in a very low intensities. This may be due to the well dispersed small amount of Keggin structure on the titania surface without any structural changes. The SEM and EDX analysis data revealed presence of HPW incorporated with TiO<sub>2</sub> nanoparticles in all the prepared samples. The FTIR inspections confirmed interaction between HPW and TiO<sub>2</sub> with remaining HPW structure unchanged.

## ACKNOWLEDGEMENTS

Authors would express their thanks to the Research Vice-Presidency of Science and Research Branch, Islamic Azad University and Iranian Nanotechnology Initiative (Govt. of Iran) for their support and encouragements.

## REFERENCES

- [1] Pope. M.T., Muller. A. (1991). Polyoxometalate Chemistry: An Old Field with New Dimensions in Several Disciplines. *Angew. Chem. Int. Ed. Engl.*, 30, 34-39.
- [2] Katsoulis. D.E.(1998). A Survey of Applications of Polyoxometalates., *Chem. Rev.* 98, 359-365.
- [3] Yamase. T.(1998). Photo- and electrochromism of polyoxometalates and related materials. *Chem. Rev.* 98, 307-315.
- [4] Klmpere. W.E., G.G. Wall .(1998). Polyoxoanion Chemistry Moves toward the Future: From Solids and Solutions to Surfaces. *Chem. Rev.*, 98, 297-311.
- [5] Misono. M. (1987). Heterogeneous catalysis by heteropoly compounds of molybdenum

- and tungsten., *Catal. Rev.-Sci. Eng.*, 29, 269-275.
- [6] Rafiee. E., Rashidzadeh.S., Azad.A., (2007). Silica-supported heteropoly acids: Highly efficient catalysts for synthesis of  $\alpha$ -aminonitriles, using trimethylsilyl cyanide or potassium cyanide. *J. Mol. Catal. A.*, 261 49–52.
- [7] Mizuno N, Misono. (1998). Heterogeneous catalysis. *Chem Rev.*, 98,199–218.
- [8] (a) Molinari. A., Amadelli. R., Andreotti. L., Maldotti. A. (1999). Heterogenous catalysis for synthesis purposes: Oxygenation of Cyclohexane with H<sub>3</sub>PW<sub>12</sub>O<sub>40</sub> an (Nbu<sub>4</sub>O)<sub>4</sub>W<sub>10</sub>O<sub>32</sub> Supported on silica. *J. Chem. Soc., Dalton Trans.*, 1203-1204; (b) Maldotti. A., Molinari. A., Varani. G., Lenarda. M., Storaro. L., Bigi. F., Maggi. R., Mazzacani. A., Sartori. G. (2002). Immobilization of (n-Bu<sub>4</sub>N)<sub>4</sub>W<sub>10</sub>O<sub>32</sub> on mesoporous MCM-41 and amorphous silicas for photocatalytic oxidation of cycloalkanes with molecular oxygen. *J. Catal.*, 209, 210; Maldotti. A., Amadelli. R., Vital. I., Borgatti. L., Molinari. A. (2003). CH<sub>2</sub>Cl<sub>2</sub>-assisted functionalization of cycloalkenes by photoexcited (nBu<sub>4</sub>N)<sub>4</sub>W<sub>10</sub>O<sub>32</sub> heterogenized on SiO<sub>2</sub>. *J. Mol. Catal. A: Chem.*, 204–205, 703-704; (d) Molinari. A., Varani. G., Polo. E., Vaccari. S., Maldotti. A. (2007). Photocatalytic and catalytic activity of heterogenized W<sub>10</sub>O<sub>32</sub>- in the bromide assisted bromination of arenes and alkenes in the presence of oxygen. *J. Mol. Catal. A: Chem.*, 262,156; (e) Maldotti. A., Molinari. A., Bigi. F. (2008). Selective photooxidation of diols with silica bound W<sub>10</sub>O<sub>32</sub>-. *J. Catal.*, 253,312-316.
- [9] Guo. Y., Li. D., Hu. C., Wang. E., Wang. Y., Zhou. Y., Feng. S. (2001). Photocatalytic Degradation of Aqueous Organochlorine Pesticide on the Layered Double Hydroxide Pillared by Paratungstate A ion, Mg<sub>12</sub>Al<sub>6</sub>(OH)<sub>36</sub>(W<sub>7</sub>O<sub>24</sub>)•4H<sub>2</sub>O., *Appl. Catal. B: Environ.*, 30,337-349.
- [10] Ozer. R.R., Ferry. J.L. (2002). Photocatalytic Oxidation of Aqueous 1,2-Dichlorobenzene by Polyoxometalates Supported on the NaY Zeolite. *J. Phys. Chem. B.*, 106 ,4336-4339.
- [11] Anandan. S., Ryu. S.Y., Cho. W., Yoon . M. (2003). Heteropolytungstic acid (H<sub>3</sub>PW<sub>12</sub>O<sub>40</sub>)—encapsulated into the titanium-exchanged HY (TiHY) zeolite: a novel photocatalyst for photoreduction of methyl orange. *J. Mol. Catal. A: Chem.*, 195, 201-208.
- [12] Jiang. C., Guo. Y., Hu. C., C. Wang, D. Li . (2004). Photocatalytic degradation of dye naphthol blue black in the presence of zirconia-supported Ti-substituted Keggin-type polyoxometalates. *Mater. Res. Bull.*, 39, 251-261.
- [13] Yang. Y., Wu. Q., Guo. Y., Hu, C. Wang E., (2005). Efficient degradation of dye pollutants on nanoporous polyoxotungstate–anatase composite under visible-light irradiation *J. Mol. Catal. A: Chem.*, 225, 203-212.
- [14] Shen H.-Y., Mao H.-L., Ying L.-Y., Xia Q.-H. (2007). Photocatalytic selective aerobic oxidation of alcohols to aldehydes and ketones by HPW/MCM-41 in ionic liquids. *J. Mol. Catal. A: Chem.*, 276, 73-79.
- [15] Colmenares Juan Carlos, Aramendia Maria A., Marinas Alberto, Jose M. Marinas, Francisco J. Urbano .(2010). Titania nanophotocatalysts synthesized by ultrasound and microwave methodologies: Application in depuration of water from 3-chloropyridine. *J. Mol. Catal. A: Chem.*, 331, 58–63
- [16] Tsakiridis. P.E., Oustadakis. P., Katsiapi. A., Perraki. M., Agatzini-Leonardou , S. (2011). Synthesis of TiO<sub>2</sub> nano-powders prepared from purified sulphate leach liquor of red mud. *J. Haz. Mat.*, 194, 42–47.

- [17] Rafiee. E., Paknezhad. F., Shahebrahimi. Sh., Joshaghani. M., Eavani. S., Rashidzadeh. S. (2008). Acid catalysis of different supported heteropoly acids for a one-pot synthesis of  $\beta$ -acetamido ketones. *J. Mol. Catal. A: Chem* , .282, 92–98.
- [18] Han Zhiyue, Zhang Jingchang, Yang Xiuying, Zhu Hong, Cao Weiliang. (2010). Synthesis and photoelectric property of poly (3-octylthiophene)/ titanium dioxide nano-composite material. *J.Mater Sci: Mater Electron* 21:554–561.
- [19] Rafiee. E., Mahdavi. H., Eavani. S., Joshaghani. M., Shiri. F., (2009), Catalytic activity of tungstophosphoric acid supported on carriers of diverse acidity in the synthesis of enamines, *Applied Catalysis A: General* 352, 202–207.

Cite this article as: M. Seyedsadjadi *et al.*:  
Incorporation of 12-tungstophosphoric acid in  
Titania spheres and fabrication of core-shell  
Polyoxotungstate/Titania nanostructures.  
*Int. J. Nano Dimens.* 5(2): 105-112, Spring 2014